**Atmospheric
Chemistry
and Physics**

The CO_2 tracer clock for the Tropical Tropopause Layer

**S. Park[1], R. Jiménez[1], B. C. Daube[1], L. Pfister[2], T. J. Conway[3], E. W. Gottlieb[1], V. Y. Chow[1], D. J. Curran[1],
D. M. Matross[1,*], A. Bright[1], E. L. Atlas[4], T. P. Bui[2], R.-S. Gao[5], C. H. Twohy[6], and S. C. Wofsy[1]**

[1]Department of Earth and Planetary Sciences and the Division of Engineering and Applies Sciences, Harvard University,
Cambridge, Massachusetts 02138, USA
[2]NASA, Ames Research Center, Moffett Field, California 94035, USA
[3]NOAA, Earth System Research Laboratory, Boulder, Colorado 80305, USA
[4]University of Miami, Rosenstiel School of Marine and Atmospheric Science, Miami, Florida 33149, USA
[5]NOAA Aeronomy Laboratory, Boulder, Colorado 80303, USA
[6]Oregon State University, College of Oceanic and Atmospheric Science, Corvallis, Oregon 97331, USA
[*]now at: Department of Environmental Science Policy and Management, University of California, Berkeley, California
94720, USA

Abstract. Observations of CO_2 were made in the upper troposphere and lower stratosphere in the deep tropics in order to determine the patterns of large-scale vertical transport and age of air in the Tropical Tropopause Layer (TTL). Flights aboard the NASA WB-57F aircraft over Central America and adjacent ocean areas took place in January and February, 2004 (Pre-AURA Validation Experiment, Pre-AVE) and 2006 (Costa Rice AVE, CR-AVE), and for the same flight dates of 2006, aboard the Proteus aircraft from the surface to 15 km over Darwin, Australia (Tropical Warm Pool International Cloud Experiment, TWP-ICE). The data demonstrate that the TTL is composed of two layers with distinctive features: (1) *the lower TTL*, 350–360 K (potential temperature(θ); approximately 12–14 km), is subject to inputs of convective outflows, as indicated by layers of variable CO_2 concentrations, with air parcels of zero age distributed throughout the layer; (2) *the upper TTL*, from $\theta=\sim360$ K to ~390 K (14–18 km), ascends slowly and ages uniformly, as shown by a linear decline in CO_2 mixing ratio tightly correlated with altitude, associated with increasing age. This division is confirmed by ensemble trajectory analysis. The CO_2 concentration at the level of 360 K was 380.0(±0.2) ppmv, indistinguishable from surface site values in the Intertropical Convergence Zone (ITCZ) for the flight dates. Values declined with altitude to 379.2(±0.2) ppmv at 390 K, implying that air in the upper TTL monotonically ages while ascending. In combination with the winter slope of the CO_2 seasonal cycle (+10.8±0.4 ppmv/yr), the vertical gradient of –0.78 (±0.09) ppmv gives a mean age of 26(±3) days for the air at 390 K and a mean ascent rate of 1.5(±0.3) mm s^{-1}. The

TTL near 360 K in the Southern Hemisphere over Australia is very close in CO_2 composition to the TTL in the Northern Hemisphere over Costa Rica, with strong contrasts emerging at lower altitudes (<360 K). Both Pre-AVE and CR-AVE CO_2 observed unexpected input from deep convection over Amazônia deep into the TTL. The CO_2 data confirm the operation of a highly accurate tracer clock in the TTL that provides a direct measure of the ascent rate of the TTL and of the age of air entering the stratosphere.

1 Introduction

The Tropical Tropopause Layer (TTL) is the transition region between the troposphere and stratosphere (Folkins et al., 1999; Highwood and Hoskins, 1998) and the dominant source region of air entering the stratosphere. The lower and upper boundaries are generally defined as the level of minimum potential temperature lapse rate (~10–12 km altitude, approximately potential temperature ~350 K) and of the cold point at ~17–19 km (near ~380 K) (Gettelman and Forster, 2002). Understanding of the origins and transport processes for the air in the TTL is key to defining the inputs of short-lived and long-lived compounds into the stratosphere, e.g., those associated with stratospheric ozone depletion, and to understanding the mechanisms that control humidity and cloudiness in the TTL and stratosphere.

Satellite observations and 2-D or 3-D transport models provide a general picture of the TTL, but typically cannot resolve spatial variations within the layer. Hence, in situ measurements of tracer species such as CO and O_3 (e.g., Folkins et al., 2002a; Folkins et al., 2006; Hoor et al., 2002; Randel et

Correspondence to: S. C. Wofsy
(swofsy@deas.harvard.edu)
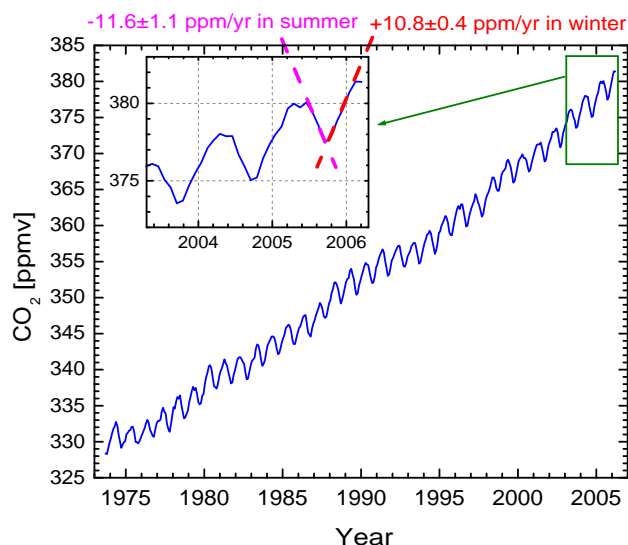
Fig. 1. The global CO_2 seasonal cycle from (CO_2-MLO + CO_2-SMO)/2 (Boering et al., 1996) using ESRL data (Conway et al., 1994, updated by T. Conway). The inset shows as expanded time axis with the CR-AVE time period.

al., 2007; Schoeberl et al., 2006), water vapor (e.g., Brewer, 1949; Folkins et al., 2002b; Stohl et al., 2003), and CO_2 (e.g., Andrews et al., 1999; Andrews et al., 2001a; Boering et al., 1995; Fischer et al., 2002) have been the principal tools for studying the radiative, chemical, and dynamical properties of the TTL. Data for CO_2, already used to infer the mean age of air and the age spectrum of the lower stratosphere (e.g., Andrews et al., 2001a; Andrews et al., 2001b; Boering et al., 1996), can be particularly useful in the TTL. The CO_2 mixing ratio has a well-measured trend over time, upon which is superimposed a pronounced seasonal cycle. Boering et al. (1996) suggested that the average data for CO_2 at Mauna Loa (MLO) and Samoa (SMO) (Fig. 1) was a suitable approximation of the mean CO_2 in air lofted into the upper troposphere ("*CO_2 Index*", data updated by T. Conway). The seasonal rates of change of the *Index* appear capable of providing a very sensitive "CO_2 clock" for tracing the time since air left the near-surface environment and entered the TTL. The seasonal slope in January and February ($+10.8\pm0.4$ pmv yr^{-1}, see inset of Fig. 1 with expanded time axis) implies an increase of ~28–30 ppb day^{-1}. The Harvard CO_2 instrument has resolution of 50–100 ppb (Daube et al., 2002) enabling it to distinguish mean age differences as short as 2–3 days. This paper presents high-resolution, in situ observations of CO_2 concentrations to define the residence time and ascent rates for air in the TTL. We identify source regions for air entering the TTL and provide definitive time scales for TTL transport process by developing and validating the concept of the CO_2 tracer clock. The CO_2 measurements in the TTL were carried out on a series of flights of the NASA WB-57F aircraft over Costa Rica and adjacent

ocean areas during the NASA Pre-Aura Validation Experiment (Pre-AVE) and Costa Rica AVE (CR-AVE) in January and February, 2004 and 2006, respectively. A large number of other tracer and meteorological measurements were made on the aircraft, providing important information on the chemical and dynamical context of the sampled air. The AVE missions give the first comprehensive tracer data for the TTL. During the same flight period as CR-AVE, we also obtained in situ CO_2 data on board the Proteus aircraft, from the Planetary Boundary Layer (PBL) up to 15 km over Darwin (12° S), Australia (part of Tropical Warm Pool International Cloud Experiment, TWP-ICE). These data allow the inter-hemispheric comparison of CO_2 composition of the TTL. We present our extensive CO_2 observations of the TTL in the context of the characteristics of TTL structure and transport. First, instrumental information is given in the following section. In Sect. 3.1, the CO_2 vertical profiles from CR-AVE are shown in potential temperature coordinates. In Sect. 3.2, we present the observed variations/anomalies in the CO_2 profiles in the lower TTL region below 360 K that can be explained mainly by influence of local and/or remote convective inputs. In Sect. 3.3, we discuss the validity of the CO_2 tracer clock in the upper TTL region between 360 and 390 K and provide a direct measure of the mean vertical ascent rate and mean age of air transiting the TTL and entering the stratosphere.

2 Measurements

Measurements of CO_2 mixing ratios on the NASA WB-57F aircraft and on the Proteus aircraft were made using nondispersive infrared absorption CO_2 analyzers flown in many previous experiments (see Daube et al., 2002, for details). The instruments are calibrated often in flight, and have demonstrated a long-term precision of 0.1 ppmv (Boering et al., 1995). The standards are calibrated directly against CO_2 world standards from the National Oceanic and Atmospheric Administration/Earth System Research Laboratory (NOAA/ESRL), and thus are directly comparable to surface data from the ESRL global network, with accuracy better than 0.1 ppmv. Our analysis uses data for potential temperature, ozone, and condensed water content (CWC) from other sensors on the WB-57F, and CH_4 mixing ratios from Pre-AVE whole air samples. Air temperature and pressure were measured by the Meteorological Measurement System (MMS) on board the aircraft, with the reported precision and accuracy of ±0.1 K and ±0.3 K, respectively, for temperature, and ±0.1 hPa and ±0.3 hPa, for pressure (Scott et al., 1990). These parameters were used to derive potential temperate with an uncertainty of ~2 K. In situ ozone measurements were made by the NOAA Dual-Beam UV Absorption Ozone Photometer (Proffitt and McLaughlin, 1983). At a 1-s data collection rate, measurement precision is ±0.6 ppbv (STP) and average uncertainty is ~±5%. The Cloud Spectrometer and Impactor (CSI –
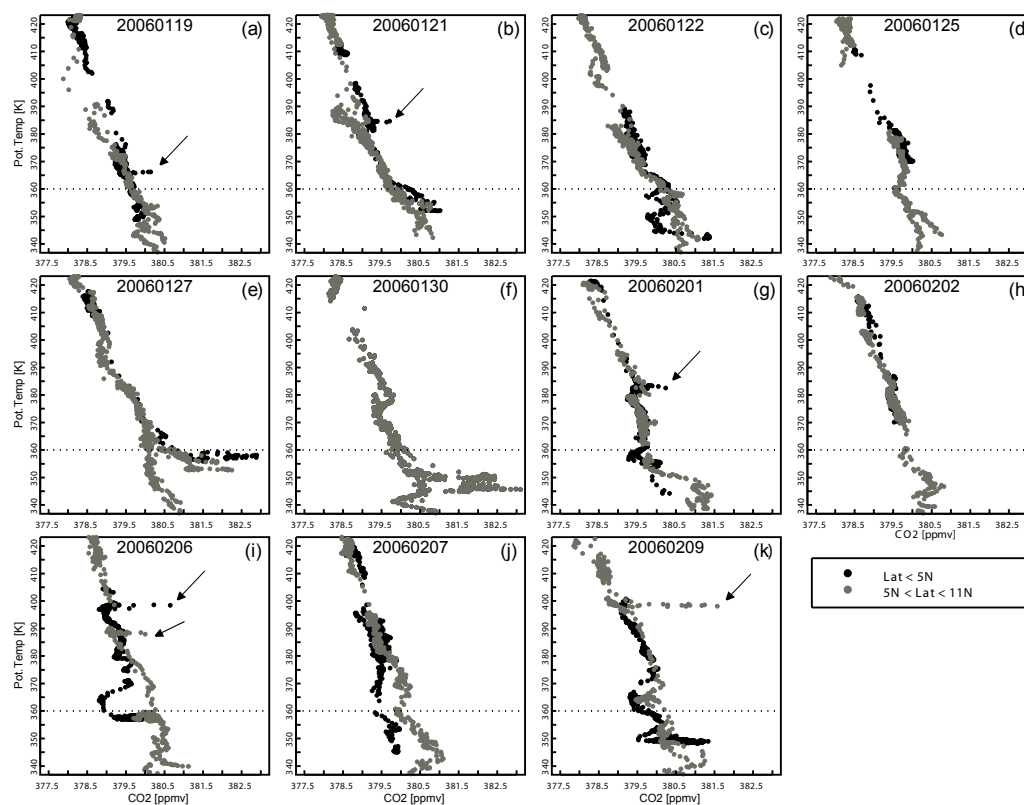
Fig. 2. Vertical profiles of CO$_2$ from 11 scientific flights in the tropics (<11° N) during CR-AVE. Data from the deep tropics less than 5° N are given in black and 5–11° N in gray. Note aircraft contrails are readily detected (marked by arrows). Horizontal dotted lines denote the level of 360 K. **(a)**–**(k)** represent the flights on 19, 21, 22, 25, 27, and 30 January and 1, 2, 6, 7, and 9 February, 2006.

Droplet Measurement Technologies) is based on the technology of the Counterflow Virtual Impactor (CVI) (Twohy et al., 1997) and was used to measure total condensed water content in the range from 0.001 to 5 g m^{-3}. Whole air samples were collected with the National Center for Atmospheric Research (NCAR) Whole Air Sampler (WAS) (Flocke et al., 1999). Mixing ratios of CH$_4$ on the WAS samples were measured using a Hewlett Packard model 5890 gas chromatograph fitted with a flame ionization detector (GC-FID). Calibration was made against a 0.913±0.01 and a 1.19±0.01 μmol/mol NIST-certified SRM 1658a reference gas. Measurement precision is ±10 ppbv and accuracy is ±20 ppbv.

3 Results and discussions

3.1 CO$_2$ observations from CR-AVE

Measurements of CO$_2$ during CR-AVE are plotted in potential temperature (θ) coordinates in Fig. 2. Data from 11 science flights that sampled in the deep tropics, south of 11° N are grouped by latitude, less than 5° N in black and 5–11° N in gray, flight-by-flight. For all 11 profiles, the observed CO$_2$ mixing ratios in general decline with increasing potential

temperature (i.e., altitude) throughout the observed range of ∼330–430 K. Aircraft contrails (denoted by arrows in Fig. 2) and associated inputs of CO$_2$ from combustion were readily detected.

Most of the CO$_2$ vertical profiles for potential temperature <∼360 K reveal considerable variations with either *low* CO$_2$ bulges or *high* CO$_2$ spikes, or both (for example, see the flights of 22, 27, and 30 January and 1, 6, 7, and 9 February). Variability is much less above 360–370 K. For the flights on 6, 7, and 9 February (Figs. 2i, j, and k, respectively), *low* CO$_2$ bulges are most apparent, by ∼1.5 ppmv at ∼360 K, at the southern end of the flights, i.e., only latitudes less than 5° N. Figure 3 shows that these bulges correspond perfectly with elevated O$_3$, a stratospheric tracer, implying substantial intrusion of lower stratospheric air at the southern end of the flights for those dates: this intrusion brought older, stratospheric levels of CO$_2$. However, other *low* CO$_2$ excursions from other flights do not pick up any corresponding feature in O$_3$ (e.g., a *low* CO$_2$ excursion marked by a circle in Fig. 3c) and these are discussed further in Sects. 3.2.2 and 3.2.3 below.

In contrast to the lower TTL below ∼360 K, CO$_2$ profiles for potential temperature between ∼360–390 K form a
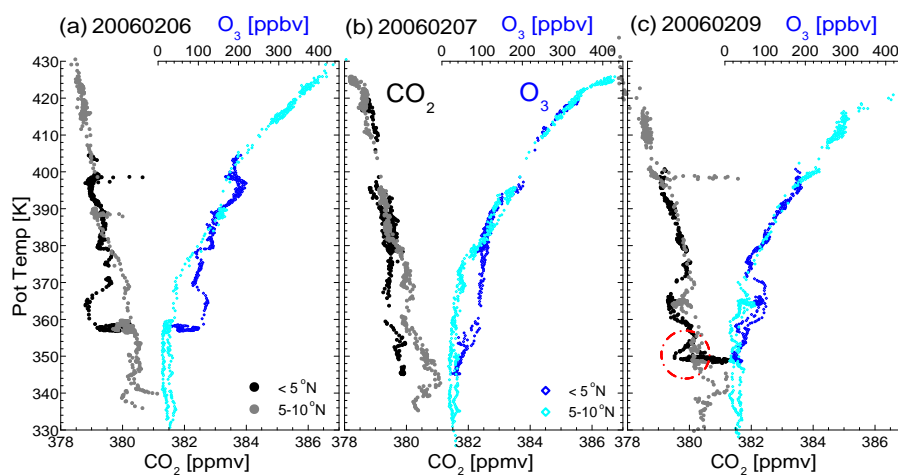
Fig. 3. Vertical profiles of CO_2 (denoted by solid dots) and O_3 (by blue diamonds) on 6 (**a**), 7 (**b**), and 9 (**c**) February. *Low CO₂ bulges* from <5° N are responding to high ozone signals, suggesting stratospheric air input. Note dotted circle on Feb. 9 marks the air mass influenced from deep convection over Amazon basin, discussed in Sect. 3.2.2.

compact, linear line with a negative slope in most flights. The monotonic decline in the mixing ratio is very significant, indicating that air is aging with altitude since the seasonal cycle is on the rising branch in boreal winter (see Fig. 1). Differences in some of the CO_2 profiles between <5° N and 5–11° N, from the minimum temperature level (i.e., ∼380 K) to ∼390–400 K may also be discernable (see Figs. 2a, b and c). Slightly lower CO_2 values at 5–11° N seem to reflect influence of horizontal mixing between the tropical and midlatitude stratospheric "overworld" (defined as the region above ∼380 K), but profiles at <5° N were not affected. Differences between <5° N and 5–11° N disappear above ∼400 K, the level where air enters the "tropical pipe". At these altitudes, a transport barrier in the 15–30° N latitude range restricts mixing of midlatitude air into the tropics (Neu and Plumb, 1999; Plumb, 1996).

The CO_2 profiles in potential temperature coordinate suggest that the TTL is composed of two layers with the distinctive features. The lower TTL, up to the level of ∼360 K (14–15 km), exhibits profiles with considerable daily and latitudinal variations. In Sect. 3.2, we detail how these observed anomalies in the profiles can be explained by convective influence. The upper TTL ranging from ∼360 K to ∼390 K (17–18 km; slightly above the tropical tropopause) is by contrast characterized by a linear decline and a compact correlation between altitude and CO_2 mixing ratio, regardless of flight date and latitudinal range. We discuss in Sect. 3.3 the implication of this observation for interpreting air ascending motion of the region.

3.2 Lower TTL below 360 K

We show here that the CO_2 variations observed in the lower TTL are indicating the influences of (1) local convection near

Central America, (2) convective input from Amazônia, and (3) remote, deep convection over south central/western Pacific. We demonstrate that this explanation is entirely consistent with the analyses from condensed water content data, back trajectories, and CH_4 measurements.

3.2.1 Local convection

For the flights on 27 and 30 January (see Figs. 2e and f), we measured *high* CO_2 spikes of 2–3 ppmv between 12–13 km (i.e., ∼350–360 K). The CO_2 maxima are about 383 ppmv which corresponds to the mixing ratio of the near-surface in the northern tropics near Costa Rica. The CO_2 monthly averages at Barbados (RPB, 13° N 59° W), Key Biscayne (KEY, 25° N 80° W), St. David's head (BME, 32° N 64° W) and Tudor Hill (BMW, 32° N 64° W) ESRL stations reach up to 381.8–384.5 ppmv in January, 2006. This implies a rapid injection of undiluted northern hemisphere tropical boundary layer air by deep convection to the level of 350–360 K. Figures 4a and b show typical CR-AVE flight segments on 27 and 30 January 2006. Note the correspondence with condensed water content in the outflow of a deep convective cloud, and the elevated CO_2, which is illustrating that we sampled wet air with high CO_2 just outside a convective cloud. Hence, cloud outflows constituting nearly undiluted air from the local boundary layer are clearly observed as elevated CO_2 in a number of instances, for potential temperatures lower than ∼360 K.

3.2.2 Input from convection over Amazônia

The unexpected, but most interesting finding in the CO_2 data from Pre-AVE in 2004 was the anomalously strong *low* CO_2 signals near 350 to 360 K of the vertical profiles (Fig. 5a). These appear to be explained by the convective input from

Amazon basin into the TTL (see Figs. 6a and b for back trajectories). Amazônian influence in the TTL was also observed in the CR-AVE CO_2. As seen in Fig. 3c, a *low* CO_2 excursion is apparent near 350 K in the profile at <5° N on 9 February, whereas O_3 and CO gave no corresponding hint of this feature. An independent analysis of back trajectory for CR-AVE (see Fig. 7) showed that this is a 2-day old air mass from Amazônia.

Other possible explanations for this low-CO_2 feature can be rejected. If deep convection reached up to the tropopause near 380 K, younger air in the upper TTL would have more CO_2 than older air in the lower TTL, as observed, but also CO should increase with altitude, reflecting near-surface influence at the upper level. But CO concentrations decline with altitude, as shown in Fig. 5c. Another possibility might be stratospheric input, but we could not find any indication of elevated ozone (see Fig. 5).

In contrast to ozone and CO, the CH_4 profile in Fig. 5d shows an anomaly, with *high* CH_4 near 360 K corresponding to *low* CO_2 signals. The concentrations of CH_4 in Amazônia are about 100 ppb higher than the global mean near the equator (J. Miller, personal communication, 2006), consistent with the observed enhancement. During the transition from dry to wet season in late-January to early February, deep convection over Amazônia increases, occurring primarily in the afternoon (Liu and Zipser, 2005; Machado et al., 2004) when CO_2 values are low (as low as ∼375 ppmv; L. Hutyra, personal communication, 2006) due to the forest uptake. Thus deep convection over Amazônia brings CO_2-depleted air to the TTL in contrast to inputs from local convection discussed in Sect. 3.2.1 above. There is little biomass burning at this season, hence no enhancement is observed in CO.

We note that input to the TTL by deep convection over Amazônia was evident in CO_2 observations in both Pre-AVE and CR-AVE, suggesting that this process may be typical of the January–February time period. Amazônian influence in the TTL is potentially very important for the chemistry of the TTL and lower stratosphere, in terms of excess reactive hydrocarbons and CH_4 that the convective input must carry to the TTL. This finding highlights the importance of multiple-tracer measurements including CO_2, CH_4 and CO, since these tracer observations together can provide the capability to distinguish source air in the TTL from deep convection over tropical forests versus the ocean and then to infer a quantitative measure of these influences. Quantitatively defining source regions that supply trace gases and H_2O to the TTL would potentially allow us to address long-term changes in the humidity and aerosol content of the TTL and lower stratosphere.

3.2.3 Influence of remote convection over the Western/Central Pacific

Flights on 22 January and 1 February (see Figs. 2c and g) recorded *low* CO_2 excursions observed near 350 and 355 K
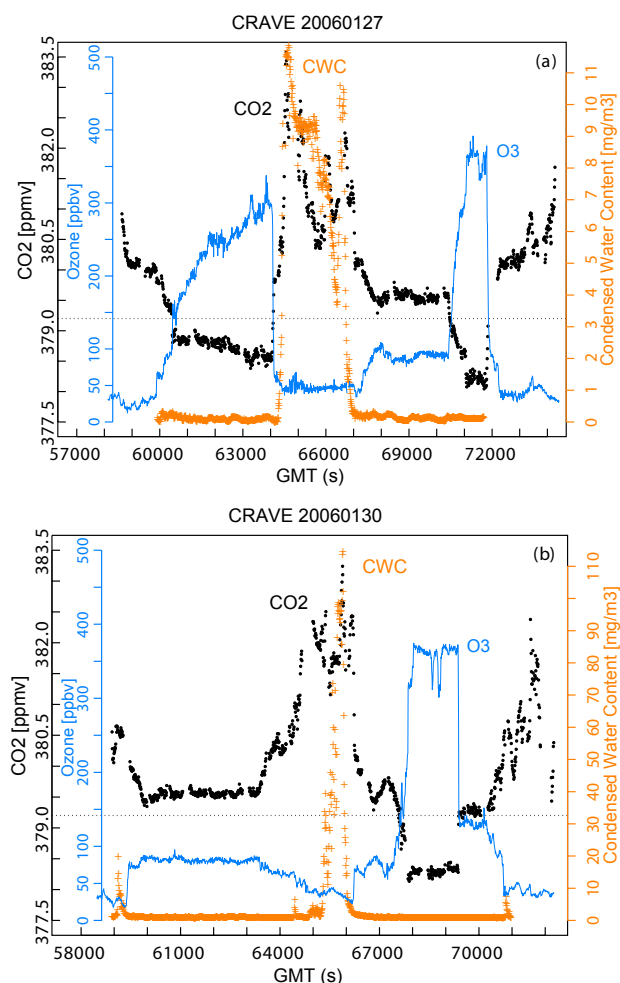

Fig. 4. Flight segments for CO_2, O_3 and condensed water content (CWC) **(a)** on 27 January and **(b)** on the 30. The CO_2 peaks that correspond to CO_2 spikes in the vertical profiles (Figs. 2e and f), are clearly responding to enhanced condensed water content in the outflow of convective clouds. Note high O_3 and low CO_2 mixing ratios on the stratospheric side. Horizontal dotted line represents a CO_2 level at the tropopause. Black, solid dots give CO_2, blue lines for O_3, and orange, cross symbols for CWC.

that cannot be explained by either local convection (CO_2 would be *high*) nor by Amazônian input, since CH_4 is *low*. The origins of low-CO_2 air were examined using 10-day back trajectory analysis that tracked the air envelope surrounding ±0.5 km from the aircraft track to calculate statistics of air clusters influenced by convection for the last 10 days (Pfister et al., 2001). A significant fraction of air cluster points from those low-CO_2 air masses shows non-zero convective influence in the central Pacific, i.e., the northern part of the South Pacific Convergence Zone (SPCZ), off the northeast Australian coast, and in the New Guinea/Indonesia region. Evidently we sampled remnant air from convection
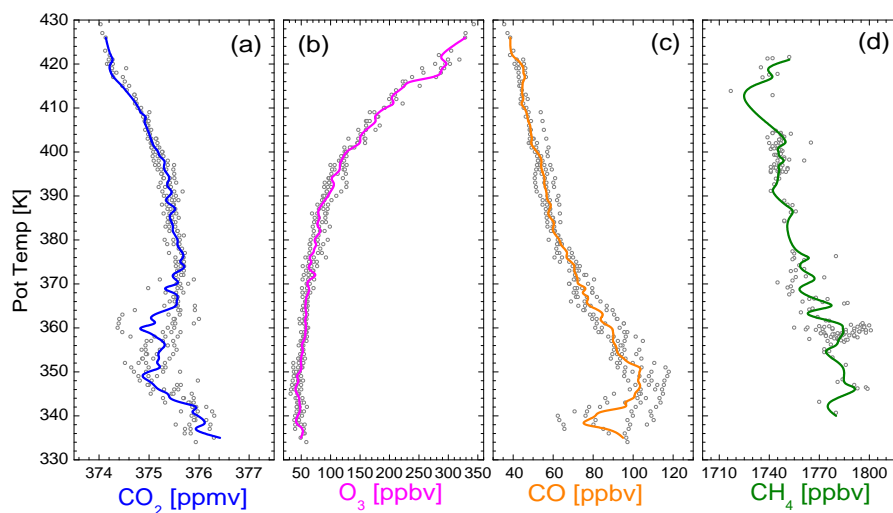
Fig. 5. Pre-AVE **(a)** CO_2, **(b)** O_3, **(c)** CO, and **(d)** CH_4 observations. Empty circles represent averages in 1-K intervals of potential temperature for each flight on 24, 27, 29, and 30 January 2004. 1-K averages including all the flights are denoted by solid lines. Note that *low* CO_2 values found at ∼350 and 360 K reflect deep convective input over Amazônia, carrying reduced-CO_2 air due to forest uptake.
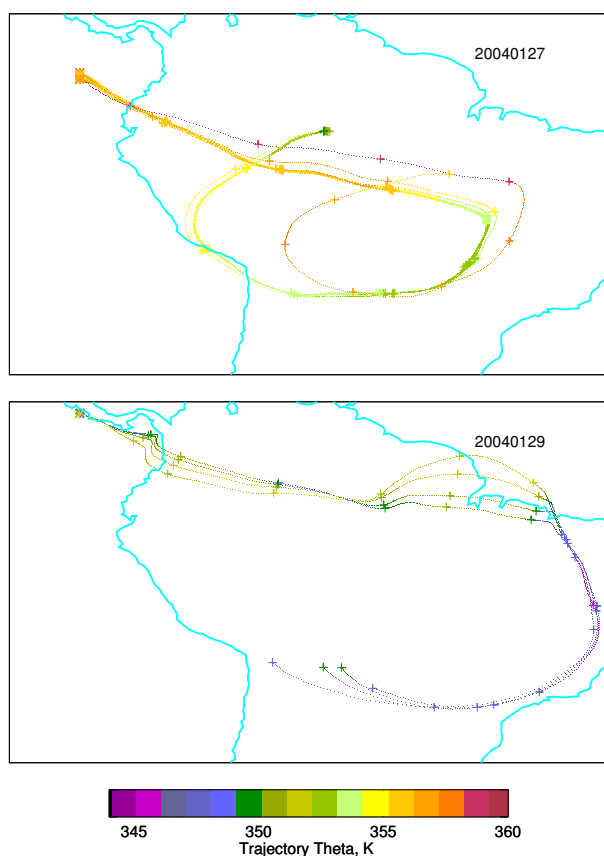
Fig. 6. Back trajectories that trace **(a)** the low-CO_2 air masses at ∼360 K of the flight on 27 January and **(b)** the air mass at ∼350 K of the flight on 29 January to Amazônia.
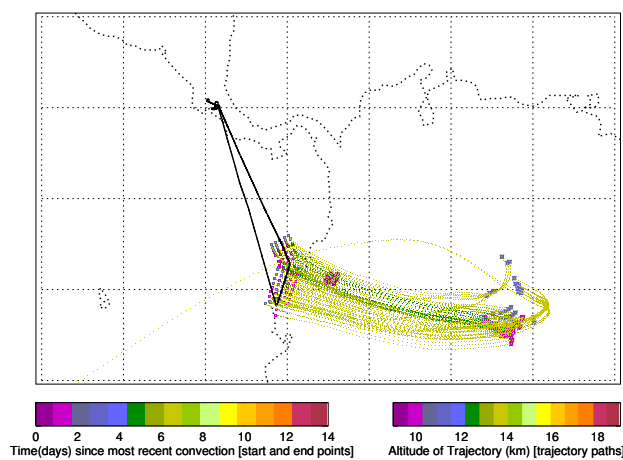

Fig. 7. Back trajectories that trace the low-CO_2 air masses at ∼350 K of the flight on 9 February 2006 to Amazon basin.

over the south central and/or western Pacific.

The CO_2 composition of air originating from the south central/western Pacific can be examined from our CO_2 data obtained during TWP-ICE. Figure 8 shows the vertical CO_2 profiles from the flights on 25, 27, and 29 January 2006, over the south western Pacific (12° S, 130° E). The Proteus aircraft sampled from near the surface (altitude of ∼1 km, ∼300 K) up to around 15-km altitude (i.e., ∼360 K). The CO_2 mixing ratio at ∼1 km was between 378.1 and 378.8 ppmv, increased to the range between 379 and 380 ppmv below ∼4 km, and then stayed nearly constant with altitude to the aircraft's ceiling. Note strong contrast with the boundary layer CO_2 composition in the northern tropics near Costa

Rica (381.8–384.5 ppmv; see Sect. 3.2.1). CO_2 measured at southern/central tropical, ESRL stations – Mahe Island (SEY, 4° S 55° E), Ascension Island (ASC, 7° S 14° W), Samoa (SMO, 14° S 170° W), Cape Grim (CGO, 40° S 144° E), and Christmas Island (CHR, 1° N 157° W), averaged 379.9 (±1.3) ppmv in January, 2006, consistent with TWP-ICE. An average of CO_2 data for the northern tropical Pacific stations, Guam (GMI, 13° N 144° E) and Mauna Loa (MLO, 19° N 155° W) was 381.4 (±0.3) ppmv. Thus, convective input will cause excursion to either *low* or *high* CO_2 in the profiles as observed for CR-AVE, depending on whether it originates from the southern tropical marine boundary layer or from nearby northern hemisphere tropical region, respectively. Hence, we infer that the *low* CO_2 excursions of CR-AVE flights on 22 January and 1 February were due most likely to remote, convective influence on the TTL of southern marine boundary layer air, in agreement with back trajectory results. It is also noted that the convective influences remained measurable for several days (i.e., ∼7–9 days; an estimate from the trajectory analysis) in the TTL, and were readily detected by CO_2.

The TWP-ICE observations revealed clear difference in CO_2 mixing ratio from the surface to the upper troposphere and lower TTL from the CR-AVE measurements shown along in Fig. 8. The difference is more likely to represent concentration gradients between the southern and northern hemispheres rather than gradients between the west and east. Note that TWP-ICE CO_2 is much closer to southern Atlantic air (e.g., 379.2 ppmv at Ascension Island, 7° S 14° W) rather than northern Pacific air (e.g. 381.6 ppmv at Guam, 13° N 144° E). Interestingly, the strong contrasts that are apparent in the upper troposphere and lower TTL region disappear near 360 K: the CO_2 composition at ∼360 K in the southern tropics over Australia is very close to that in the northern tropics over Costa Rica. This result implies that the lower TTL below 360 K is subject to convective influence from boundary layer, but a *global* CO_2 signal emerges near 360 K in the TTL, evidently the result of inter-hemispheric mixing in the Intertropical Convergence Zone (ITCZ). The average CO_2 concentration of 380.0 (±0.2) ppmv at 360 K is somewhat closer to the southern tropical boundary layer air with average of 379.9 (±1.3) ppmv, in accord with the ITCZ location in the southern hemisphere during NH winter. It suggests that we observed zero-age air occurring near 360 K during the CR-AVE time period, with dominant influence from the ITCZ in the southern/central tropics. The TWP-ICE observations and their comparison with CR-AVE highlight the importance of obtaining complete vertical profiles, including the boundary layer, in order to separate the diverse influences on the chemical composition of the TTL.
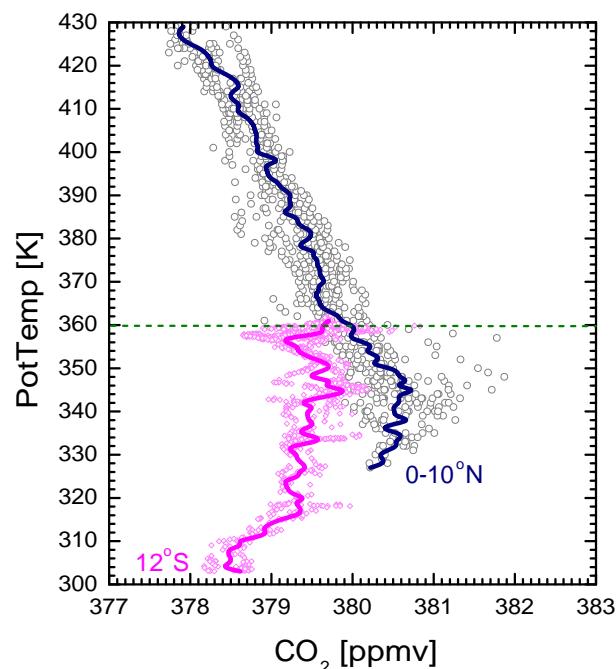

Fig. 8. Vertical profiles of CO_2 obtained during CR-AVE and TWP-ICE. TWP-ICE observations were plotted from ∼1-km to 15-km altitude on 25, 27, and 29 January 2006. The measurements were performed over the Western Pacific ocean (12° S, 130° E). All the data were averaged into 1-K intervals for each flight. Empty cycle denotes CR-AVE CO_2 and empty diamonds for TWP-ICE CO_2. The overall 1-K averages for each mission are also shown in solid lines.

3.3 Upper TTL between 360 and 390 K

3.3.1 Level of 360 K

Based on the AVE and TWP-ICE CO_2 data presented above, the level of ∼360 K is suggested as the ceiling for significant input of air by convection from the boundary layer. Back trajectory analyses to convective systems, based on the method of Pfister et al. (2001), confirm this. These analyses compute the fraction of air cluster points with non-zero convective influence for the back trajectory time (i.e., 10 and 14 days). Figure 9 shows that the convective influence fraction in 1-K average for all CR-AVE flights is concentrated mainly in the lower TTL, rapidly reducing to low values above 360 K. Back trajectories of 10 and 14 days both show the same pattern of a dramatic decrease in convective influence near 360 K. For the higher levels (near 390 K and 410 K), the occasional impact of convection seems to appear in the convective influence fraction, but not in the CO_2 profile. This convective effect might explain observed enrichment of water vapor isotopologues (e.g., Gettelman and Webster, 2005; Moyer et al., 1996; Smith et al., 2006) above and below the tropopause, which was in contrast to continuous isotopic depletion with altitude expected from Rayleigh fractionation
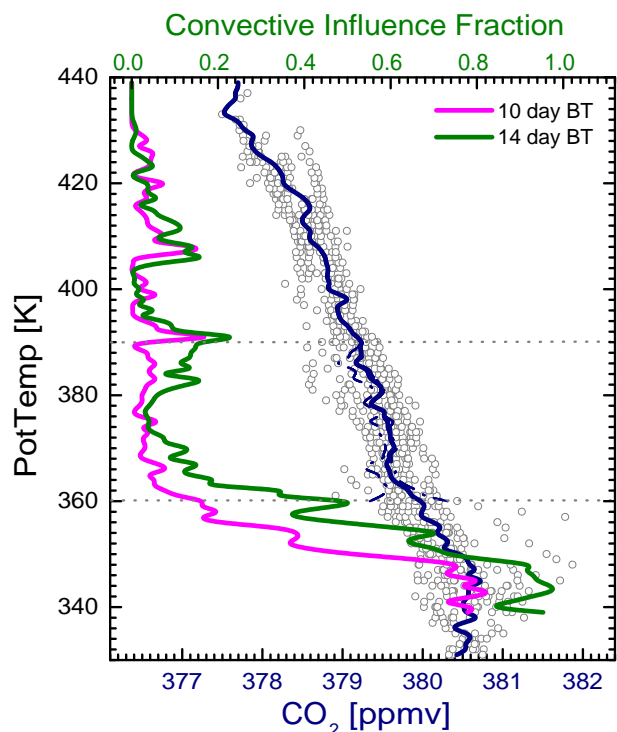
Fig. 9. Vertical profiles of CR-AVE CO_2 and fraction of air cluster points with non-zero convective influence, which was calculated by back trajectory analyses to convective systems, based on the method of Pfister et al. (2001). The pink and green lines show the 1-K averaged fraction of air clusters influenced by convection for 10 day and 14 day trajectories, respectively. To test the degree of convective influence on CO_2 distribution, CR-AVE CO_2 profile between 360 and 390 K is corrected for convective influence fraction of 10 day back trajectory. Convective air flux is assumed of two versions of CO_2 mixing ratios: 378.5 and 383 ppmv that are lower and upper limits. The corrected profiles are represented by dotted line (see text in Sect. 3.3.2). Symbols for CO_2 are same as in Fig. 8.

model while air rises. A small input of ice from evaporation can have a big effect on water vapor isotopologues, whilst the influence on CO_2 is hard to discern unless a significant fraction of the air is affected.

In addition, back trajectories of Fueglistaler et al. (2004) identified the maximum residence time of air parcels in the TTL as being at the level of ∼360 K. These authors explained that the level of zero clear sky radiative heating, where radiative balance changes from cooling to heating, occurs at ∼360 K (near 15 km), producing a so-called stagnation surface in the vertical velocity. Above that level, radiation becomes more important than convection in regulating the mass flux of air. Disappearance of the inter-hemispheric difference in CO_2 near 360 K, which is shown in Sect. 3.2.3 and Fig. 8, can also be explained by effective horizontal mixing along the stagnation level with minimum vertical velocity.

3.3.2 CO_2 tracer clock

A nearly linear decline in CO_2 mixing ratio, tightly correlated with altitude, was characteristic of the upper TTL (Fig. 2). Figures 8 and 9 showed that all CR-AVE CO_2 data form nearly identical profiles with a negative vertical gradient. Large-scale, slow upward movement and monotonic aging of air while ascending are implied by these CO_2 data, based on the rising phase of the CO_2 seasonal cycle in winter. The compact correlation of CO_2 mixing ratio with altitude (i.e., potential temperature) indicates fast horizontal mixing compared to vertical mixing. The youngest air, with near 0 age, is found at the base of the upper TTL (i.e., ∼360 K), representing a global mean CO_2 composition (see Sect. 3.2.3), as opposed to air below that level showing strong inter-hemispheric contrast in CO_2 composition (Fig. 8). Moreover, air entering the upper TTL retains imprint of the *global* seasonal cycle derived from the CO_2 *Index* (Fig. 1), as inferred by Boering et al. (1996).

These results give rise to the idea of a CO_2 "clock" for the TTL to infer a mean age and ascent rate of air using CO_2 data from the deep tropics (<11° N). The CO_2 tracer clock estimates the mean age of an air parcel in the upper TTL from the time delay between the mixing ratio observed (or inferred) at the base (∼360 K) and the mixing ratio measured in the air parcels above 360 K, with the time scale identified by the seasonal rates of change (i.e., slope of the seasonal cycle). Note that the inferred age is a true mean age representing the first moment of an age spectrum – the probability distribution function of times since air was last in contact with the surface (Hall and Prather, 1993; Waugh and Hall, 2002) – and it does not imply that all air parcels have the same history. The distribution of ages and transit times cannot be determined from CO_2 data alone. The CO_2 clock for the TTL has low resolution in the monthly time frame of July or October due to the maximum of the CO_2 *Index* in June and minimum in September, respectively.

For January/February, the value of CO_2 vertical gradient (ΔCO_2) and associated age difference between 360 and 390 K were derived in the two following ways. First, in each flight, we selected CO_2 values at 360 and 390 K and took their difference. The average and its 1σ uncertainty of the individual differences are stated as ΔCO_2 between 360 and 390 K, 0.78(±0.09) ppmv. The value of ΔCO_2 can also be obtained from the slope of the plot of CO_2 as a function of potential temperature in the range between 360 and 390 K, using a geometric mean regression which accounts for errors in both the x and y variables (Ricker, 1973). The slopes averaged 0.84(±0.29) ppmv of ΔCO_2, not statistically different from the first method. The CO_2 clock combining these CO_2 gradients with the winter slope (+10.8±0.4 ppmv/yr) of the seasonal cycle yields a mean age of air at 390 K of 26(±3) and 28(±10) days, respectively. Hence, one expects that zero-age air at 360 K would reach/pass the 390-K level in average in less than one month. Indeed, we sampled

air with CO_2 value at 390 K on 9 February identical to the 397.5 ppmv which we measured at 360 K on 14 January, exactly 26 days earlier, confirming this conclusion.

The mean ages derived from the CO_2 clock are in good agreement with recent analysis of Folkins et al. (2006). Incorporating ozonesonde O_3 data and satellite CO measurements into a radiative mass flux model with both clear sky and cloudy conditions, they reproduced the observed seasonal cycles of O_3 and CO at the tropical tropopause between 20° S and 20° N, and also calculated "an elapsed time since convective detrainment" at the altitude of 17 km, which can be interpreted as the age of air. The estimate of age was 40 days at 17 km during NH winter, but it was reduced to 25 days when modeled with correction for air mass export to extra-tropics. A trajectory analysis in the TTL incorporating radiative ascent, deep convection and zonal and meridional transport (Fueglistaler et al., 2004) also estimated one month for the average transit time from $\theta = 340$ K to 400 K, reasonably consistent with the CO_2 clock.

Our mean age values of 26($\pm$3) and 28($\pm$10) days imply mean vertical ascent rates of $\sim$1.5($\pm$0.3) and $\sim$1.4($\pm$0.5) mm s^{-1}, respectively, at θ=390 K. The inferred rates represent the spatial mean upwelling velocity in the deep tropics for NH winter rather than the global time-averaged rate, and the seasonal variation in the velocity remains to be addressed further. Nonetheless, the vertical ascent rates are notably higher than those (0.1–0.5 mm s^{-1}) derived from calculations of the meridional circulation using heating rates (e.g., Dessler, 2002; Jensen and Pfister, 2004; Randel et al., 2007). The radiative heating rates are computed with radiative transfer models using satellite and/or climatological data for radiatively active compounds, and the calculations in the TTL have large uncertainties due to the small *net* heating rates (i.e., small difference between two large numbers). Also, transient thin cirrus clouds, whose presence is difficult to detect, may alter average heating rates significantly. As estimated in Jensen et al. (1996), the radiative energy due to IR absorption by thin cirrus could lift air with a vertical ascent rate as large as $\sim$2 mm s^{-1}.

The preservation of the CO_2 seasonal trend in a compact, linear form throughout the upper TTL suggests that horizontal mixing is fairly effective compared to vertical mixing and that vertical advection dominates both vertical diffusion and the mixing in of older air from the extra-topics (i.e., the lowermost stratosphere) in this critical layer at the entry point of the stratosphere. We did not observed attenuation of the seasonal amplitudes near above 390 K (Boering et al., 1996), confirming little effect of horizontal input of older air from the extra-tropics into this deep tropics. A simple 1-D advection-diffusion model for CO_2 between 360 and 390 K was tested, shown as $\frac{\partial C}{\partial t} = -\varpi \cdot \frac{\partial C}{\partial z} + K \frac{\partial^2 C}{\partial z^2} - \gamma$, with assumption that the system is steady-state within each given time step of one day; i.e., $\partial C / \partial t = 0$. The chemical source-sink term for CO_2 is also zero. Here, vertical ascent rate,
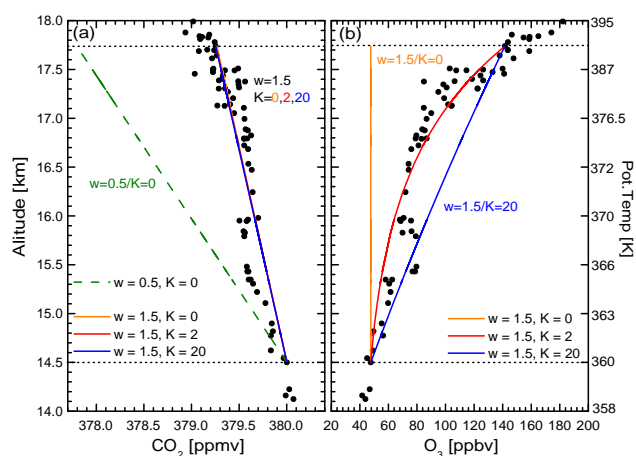
Fig. 10. **(a)** CO_2 and **(b)** ozone profiles simulated by 1-D advection-diffusion model between 360 K and 390 K for various combinations of the vertical ascent rate, ϖ and the diffusion coefficient, K. Solid dots represent 0.5-K averages of the observations. For (a), three lines with ϖ=1.5 mm s^{-1} in orange, red, and blue are overlapping on the observations, one for each choice of K=0, 2, and 20 cm^2 s^{-1}, implying that diffusion has negligible influence on the observed CO_2. The profile with ϖ=0.5 mm s^{-1} and K=0 cm^2 s^{-1} shows significant difference from both the observations and model profiles with ϖ=1.5 mm s^{-1}. The model profiles of ozone in (b) for three values of the diffusion coefficient, K are apparently distinguishable.

ϖ in m day^{-1} and the vertical diffusion coefficient, K in m^2 day^{-1} are assumed to be constant with altitude. γ denotes the rate of increase of the mixing ratio of air mass entering the upper TTL region and is 0.0294 ppmv day^{-1} estimated from the rising branch of CO_2 seasonal cycle between October 2005 to March 2006. The model calculation showed that the vertical diffusion of stratospheric air had negligible influence on observed CO_2 (see Fig. 10a). Trace influence of stratospheric air in the TTL tend to be detected by other trace gases such as O_3 and HCl (e.g., Marcy et al., 2004; Marcy et al., 2007). In contrast to CO_2, these species have very strong gradients in mixing ratio between troposphere and stratosphere, e.g., $\sim$40 ppbv at 340 K vs. $\sim$400 ppbv at 430 K for O_3 (see Fig. 3) and zero vs. $\sim$0.3 ppbv for HCl. These gases thus display small influences of stratospheric air, as illustrated by the advection-diffusion model for ozone as an example in Fig. 10b.

How much influence of recent convective injection could there be beyond the large-scale, slow ascent of the upper TTL? The vertical distribution of convective influence fraction for the back trajectories (Fig. 9) may help address this question. We examine the impact of convection on CO_2 profiles in the upper TTL by assuming the convective influence fraction of 10 day trajectory as the actual air fraction containing the most recent convective injection. We also assume two extreme cases for CO_2 in the convective air: 378.5 ppmv obtained from the surface in the TWP-ICE
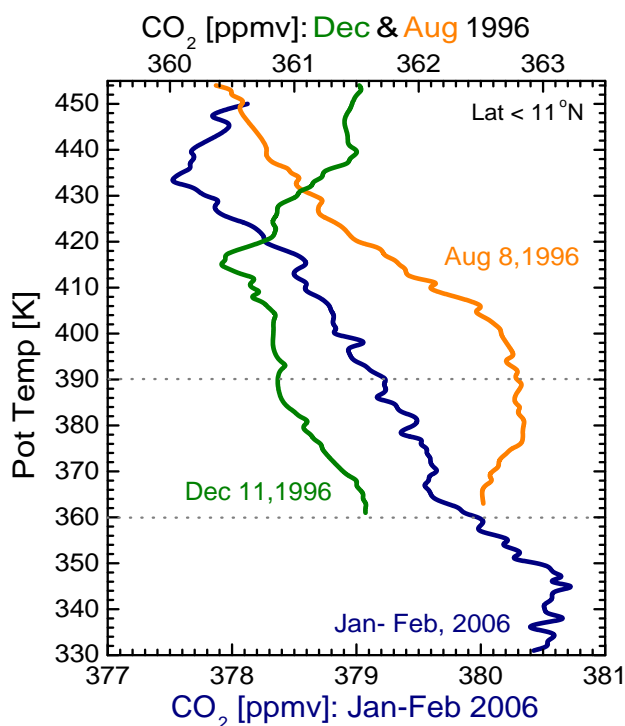
Fig. 11. Two profiles of CO_2 in the TTL from the central Pacific obtained during STRAT are shown along with CR-AVE CO_2. Data from winter (December) are remarkably consistent with data from CR-AVE. Note the reversed CO_2 gradient in August and thus operation of the CO_2 clock.

flights, and 383 ppmv from the northern tropical boundary layer. The associated change in the CO_2 mixing ratios after accounting for the convective influence fraction in each case is not statistically significant, because the input fractions are too small. The slopes for the CO_2 clock with a putative correction for convective influence, and without correction, all agree within their 1σ uncertainties, as illustrated in Fig. 9. Therefore, the small amounts of convection that might introduce in the region above 360 K would not be expected to have an observable effect on the CO_2 vertical distribution, and thus not on CO_2 clock in the region. This insensitivity results from the fact that the CO_2 clock represents the true mean age.

The operation of the CO_2 clock in the northern hemispheric summer can be tested in a preliminary way by examining CO_2 data collected during Stratospheric Tracers of Atmospheric Transport (STRAT) campaign in 1996. During STRAT, we sampled the lower tropical stratosphere and upper TTL over the central Pacific in December and August. The STRAT CO_2 data shown in Fig. 11 are all consistent with the CO_2 tracer clock, showing that the youngest air is at the base of the upper TTL and air is in slow rising above that level. Particularly, the vertical profile for August exhibited a CO_2 gradient reversed compared to December between

360 K and 390 K in STRAT or January/February in CR-AVE and Pre-AVE, consistent with the opposite phase of the seasonal cycle in NH summer (summer slope of -11.6 ppmv/yr; see Fig. 1). We expect the TC^4 measurement program scheduled in July 2007 will help complete the tracer clock concept for NH summer and provide a seasonal constraint on the vertical transport rates for the TTL. Once the vertical ascent rate and the mean age inferred from CO_2 observations are well established, these parameters provide strong constraints to help evaluate models and to help interpret satellite measurements that cannot resolve the vertical structure of the TTL.

4 Conclusions

The first extensive CO_2 data for the TTL, collected during Pre-AVE, CR-AVE, and TWP-ICE, were used to determine the average source locations for air entering the TTL and to define the time scales for air transport.

The in situ CO_2 measurements show that the TTL is composed of two layers with distinctive features: *the lower TTL* below 360 K, subject to inputs of convective outflows; and *the upper TTL* from $\sim$360 to $\sim$390 K, characterized by a compact, nearly linear decline in CO_2 mixing ratio with altitude. Observed variations in CO_2 vertical profiles for the lower TTL are explained by the episodic influence of local and/or remote convective transport. Combining data for condensed water content, CH_4, and back trajectories, we could distinguish inputs of northern hemisphere boundary layer air from Central America and adjacent waters, Amazônian air, and the remote marine boundary layer air originating from the south central/western Pacific.

In the upper TTL, the data enabled us to validate the operation of a *CO_2 tracer clock* performing in an apparently uniform manner in both hemispheres. The comparison in CO_2 composition of the TTL between CR-AVE and TWP-ICE revealed that strong contrast between the hemispheres persists from the surface to lower TTL, but seems to disappear at the level of $\sim$360 K. Therefore, air entering the upper TTL has been efficiently mixed between the hemispheres, to give a CO_2 mixing ratio very similar to the average of surface stations in the ITCZ. Observations in this study reflect limited impact of the mixing and input of convective air at the altitudes above 360 K. The level of 360 K may be considered as an *average* top of convective input from the boundary layer in the deep tropics for NH winter.

The CO_2 concentration at the level of 360 K had near zero age. Concentrations of CO_2 declined with altitude up to 390 K, implying large-scale, slow ascent and monotonic aging of air in the upper TTL. The mean age of air entering the stratosphere in NH winter was 26 ± 3 days. Chemical compounds with lifetimes shorter than $\sim$26 days are expected to be injected mainly at the 360 K level, and are unlikely to be transported into the stratosphere unless deposited above the tropopause by some other pathway, e.g.,

by the small amounts of convective air that are indicated in Fig. 9. The inferred mean vertical ascent rate in NH winter was 1.5 ± 0.3 mm s^{-1} in the upper TTL, notably higher than velocities computed from radiative heating rates using satellite and climatological data. This result implies that satellite/radar observations may tend to underestimate high, thin cirrus clouds in the TTL, among other factors that heat the air in radiative transfer models. We infer that clouds in the upper TTL are more likely to lead to radiative heating rather than cooling, since they appear to drive uplift of air. Better description of cloud fields in radiative transfer models is evidently required to reproduce the observed CO_2 "clock", and these revised models will move air more quickly through the TTL and into the stratosphere.

Edited by: R. Cohen

References

Andrews, A. E., Boering, K. A., Daube, B. C., Wofsy, S. C., Hintsa, E. J., Weinstock, E. M., and Bui, T. P.: Empirical age spectra for the lower tropical stratosphere from in situ observations of CO2: Implications for stratospheric transport, J. Geophys. Res., 104(D21), 26 581–26 596, 1999.

Andrews, A. E., Boering, K. A., Daube, B. C., Wofsy, S. C., Loewenstein, M., Jost, H., Podolske, J. R., Webster, C. R., Herman, R. L., Scott, D. C., Flesch, G. J., Moyer, E. J., Elkins, J. W., Dutton, G. S., Hurst, D. F., Moore, F. L., Ray, E. A., Romashkin, P. A., and Strahan, S. E.: Mean ages of stratospheric air derived from in situ observations of CO2, CH4, and N2O, J. Geophys. Res., 106(D23), 32 295–32 314, 2001a.

Andrews, A. E., Boering, K. A., Wofsy, S. C., Daube, B. C., Jones, D. B., Alex, S., Loewenstein, M., Podolske, J. R., and Strahan, S. E.: Empirical age spectra for the midlatitude lower stratosphere from in situ observations of CO2: Quantitative evidence for a subtropical "barrier" to horizontal transport, J. Geophys. Res., 106(D10), 10 257–10 274, 2001b.

Boering, K. A., Dessler, A. E., Loewenstein, M., McCormick, M. P., Podolske, J. R., Weinstock, E. M., and Yue, G. K.: Measurements of stratospheric carbon dioxide and water vapor at northern midlatitudes: Implications for troposphere-to-stratosphere transport, Geophys. Res. Lett., 22(20), 2737–2740, 1995.

Boering, K. A., Wofsy, S. C., Daube, B. C., Schneider, H. R., Loewenstein, M., and Podolske, J. R.: Stratospheric mean ages and transport rates from observations of carbon dioxide and nitrous oxide, Science, 274(5291), 1340–1343, 1996.

Brewer, A.: Evidence for a world circulation provided by the measurements of helium and water vapor distribution in the stratosphere, Q. J. R. Meteorol. Soc., 75, 351–363, 1949.

Daube, B. C., Boering, K. A., Andrews, A. E., and Wofsy, S. C.: A high-precision fast-response airborne CO2 analyzer for in situ sampling from the surface to the middle stratosphere, J. Atmos. Oceanic Technol., 19(10), 1532–1543, 2002.

Dessler, A. E.: The effect of deep, tropical convection on the tropical tropopause layer, J. Geophys. Res., 107(D3), 4033, doi:4010.1029/2001JD000511, 2002.

Fischer, H., Brunner, D., Harris, G. W., Hoor, P., Lelieveld, J., McKenna, D. S., Rudolph, J., Scheeren, H. A., Siegmund, P., Wernli, H., Williams, J., and Wong, S.: Synoptic tracer gradients in the upper troposphere over central Canada during the Stratosphere-Troposphere Experiments by Aircraft Measurements 1998 summer campaign J. Geophys. Res., 107(D8), 4064, doi:4010.1029/2000JD000312, 2002.

Flocke, F., Herman, R. L., Salawitch, R. J., Atlas, E., Webster, C. R., Schauffler, S. M., Lueb, R. A., May, R. D., Moyer, E. J., Rosenlof, K. H., Scott, D. C., Blake, D. R., and Bui, T. P.: An examination of chemistry and transport processes in the tropical lower stratosphere using observations of long-lived and short-lived compounds obtained during STRAT and POLARIS, J. Geophys. Res., 104(D21), 26 625–26 642, 1999.

Folkins, I., Loewenstein, M., Podolske, J., Oltmans, S. J., and Proffitt, M.: A barrier to vertical mixing at 14 km in the tropics: Evidence from ozonesondes and aircraft measurements, J. Geophys. Res., 104(D18), 22 095–22 102, 1999.

Folkins, I., Braun, C., Thompson, A. M., and Witte, J.: Tropical ozone as an indicator of deep convection, J. Geophys. Res., 107(D13), 4184, doi:4110.1029/2001JD001178, 2002a.

Folkins, I., Kelly, K. K., and Weinstock, E. M.: A simple explanation for the increase in relative humidity between 11 and 14 km in the tropics, J. Geophys. Res., 107(D23), 4736, doi:4710.1029/2002JD002185, 2002b.

Folkins, I., Bernath, P., Boone, C., Lesins, G., Livesey, N., Thompson, A. M., Walker, K., and Witte, J. C.: Seasonal cycles of O3, CO, and convective outflow at the tropical tropopause, Geophys. Res. Lett., 33, L16802, doi:16810.11029/12006GL026602, 2006.

Fueglistaler, S., Wernli, H., and Peter, T.: Tropical troposphere-to-stratosphere transport inferred from trajectory calculations, J. Geophys. Res., 109, D03108, doi:03110.01029/02003JD004069, 2004.

Gettelman, A., and Forster, P. M. de F.: A climatology of the tropical tropopause layer, J. Meteorol. Soc. Jpn., 80, 911–924, 2002.

Gettelman, A. and Webster, C. R.: Simulations of water isotope abundances in the upper troposphere and lower stratosphere and implications for stratosphere troposphere exchange, J. Geophys. Res., 110, D17301, doi:17310.11029/12004JD004812, 2005.

Highwood, E. J. and Hoskins, B. J.: The tropical tropopause, Q. J. R. Meteorol. Soc., 124(549), 1579–1604, 1998.

Hoor, P., Fischer, H., Lange, L., Lelieveld, J., and Brunner, D.: Seasonal variations of a mixing layer in the lowermost stratosphere as identified by the CO-O 3 correlation from in situ measurements, J. Geophys. Res., 107(D5), 4044, doi:4010.1029/2000JD000289, 2002.

Jensen, E. and Pfister, L.: Transport and freeze‐drying in the tropical tropopause layer, J. Geophys. Res., 109, D02207, doi:02210.01029/02003JD004022, 2004.

Jensen, E. J., Toon, O. B., Selkirk, H. B., Spinhirne, J. D., and Schoeberl, M. R.: On the formation and persistence of subvisible cirrus clouds near the tropical tropopause, J. Geophys. Res., 101(D16), 21 361–21 376, 1996.

Liu, C. and Zipser, E. J.: Global distribution of convection pene-
trating the tropical tropopause, J. Geophys. Res., 110, D23104,
doi:23110.21029/22005JD006063, 2005.

Machado, L. A. T., Laurent, H., Dessay, N., and Miranda, I.: Sea-
sonal and diurnal variability of convection over the Amazonia: A
comparison of different vegetation types and large scale forcing
Theor. Appl. Climatol., 78(1–3), 61–77, 2004.

Marcy, T. P., Fahey, D. W., Gao, R. S., Popp, P. J., Richard, E. C.,
Thompson, T. L., Rosenlof, K. H., Ray, E. A., Salawitch, R. J.,
Atherton, C. S., Bergmann, D. J., Ridley, B. A., Weinheimer,
A. J., Loewenstein, M., Weinstock, E. M., and Mahoney, M. J.:
Quantifying Stratospheric Ozone in the Upper Troposphere with
in Situ Measurments of HCl, Science, 304, 261–265, 2004.

Marcy, T. P., Popp, P. J., Gao, R. S., Fahey, D. W., Ray, E. A.,
Richard, E. C., Thompson, T. L., Atlas, E. L., Loewenstein, M.,
Wofsy, S. C., Park, S., Weinstock, E. M., Swartz, W. H., and
Mahoney, M. J.: Measurements of trace gases in the tropical
tropopause layer, J. Atmos. Sci., accepted, 2007.

Moyer, E. J., Irion, F. W., Yung, Y. L., and Gunson, M. R.: ATMOS
stratospheric deuterated water and implications for troposphere-
stratosphere transport, Geophys. Res. Lett., 23(17), 2385–2388,
1996.

Neu, J. L. and Plumb, R. A.: Age of air in a "leaky pipe" model
of stratospheric transport, J. Geophys. Res., 104(D16), 19 243–
219 256, 1999.

Pfister, L., Selkirk, H. B., Jensen, E. J., Schoeberl, M. R., Toon,
O. B., Browell, E. V., Grant, W. B., Gary, B., Mahoney, M. J.,
Bui, T. V., and Hintsa, E.: Aircraft observations of thin cirrus
clouds near the tropical tropopause, J. Geophys. Res., 106(D9),
9765–9786, 2001.

Plumb, R. A.: A "tropical pipe" model of stratospheric transport, J.
Geophys. Res., 101(D2), 3957–3972, 1996.

Proffitt, M. H. and McLaughlin, R. L.: Fast-response dual-beam
UV-absorption ozone photometer suitable for use on strato-
spheric balloons, Rev. Sci. Instrum., 54(12), 1719–1728, 1983.

Randel, W. J., Park, M., Wu, F., and Livesey, N.: A large annual cy-
cle in ozone above the tropical tropopause linked to the Brewer-
Dobson circulation, J. Atmos. Sci., accepted, 2007.

Ricker, W. E.: Linear regression in Fishery Research, J. Fish. Res.
Board Can., 30, 409–434, 1973.

Schoeberl, M. R., Duncan, B. N., Douglass, A. R., Waters,
J., Livesey, N., Read, W., and Filipiak, M.: The carbon
monoxide tape recorder, Geophys. Res. Lett., 33, L12811,
doi:12810.11029/12006GL026178, 2006.

Scott, S. G., Bui, T. P., Chan, K. R., and Bowen, S. W.: The me-
teorological measurement system on the NASA ER-2 aircraft, J.
Atmos. Oceanic Technol., 7(4), 525–540, 1990.

Smith, J. A., Ackerman, A. S., Jensen, E. J., and Toon, O. B.: Role
of deep convection in establishing the isotopic composition of
water vapor in the tropical transition layer, Geophys. Res. Lett.,
33, L06812, doi:10.1029/2005GL024078, 2006.

Stohl, A., Bonasoni, P., Cristofanelli, P., Collins, W., Feichter, J.,
Frank, A., Forster, C., Gerasopoulos, E., Gäggeler, H., James, P.,
Kentarchos, T., Kromp-Kolb, H., Krüger, B., Land, C., Meloen,
J., Papayannis, A., Priller, A., Seibert, P., Sprenger, M., Roelofs,
G. J., Scheel, H. E., Schnabel, C., Siegmund, P., Tobler, L.,
T. Trickl, Wernli, H., Wirth, V., Zanis, P., and Zerefos, C.:
Stratosphere-troposphere exchange: A review, and what we have
learned from STACCATO, J. Geophys. Res., 108(D12), 8516,
doi:8510.1029/2002JD002490, 2003.

Twohy, C. H., Schanot, A. J., and Cooper, W. A.: Measurement of
condensed water content in liquid and ice clouds using an air-
borne counterflow virtual impactor, J. Atmos. Oceanic Tech., 14,
197–202, 1997.

Waugh, D. W. and Hall, T. M.: Age of stratospheric air: The-
ory, observations, and models, Rev. Geophys., 40(4), 1010,
doi:1010.1029/2000RG000101, 2002.